265 P85

*Beppo*SAX Observations of PKS 2155–304

Y.H. ZHANG[1], A. TREVES[1], A. CELOTTI[2], L. CHIAPPETTI[3], G. FOSSATI[4],
G. GHISELLINI[5], L. MARASCHI[6], E. PIAN[7], G. TAGLIAFERRI[5], F. TAVECCHIO[6]
[1] *Dipartimento di Scienze, Università dell'Insubria, via Valleggio 11, I-22100 Como, Italy*
[2] *International School for Advanced Studies, SISSA, via Beirut 2-4, I-34014 Trieste, Italy*
[3] *Istituto di Fisica Cosmica G.Occhialini, IFCTR/CNR, via Bassini 15, I-20133 Milano, Italy*
[4] *Department of Physics and Astronomy, Rice University, Houston, TX 77005 USA*
[5] *Osservatorio Astronomico di Brera (OAB), via Bianchi 46, I-22055 Merate, Italy*
[6] *Osservatorio Astronomico di Brera (OAB), via Brera 28, I-20121 Milano, Italy*
[7] *Osservatorio Astronomico di Trieste (OAT), via G.B.Tiepolo 11, I-34131 Trieste , Italy*

ABSTRACT. We present the X-ray temporal and spectral properties of the X-ray bright blazar PKS 2155–304 from three long-looks obtained with *Beppo*SAX during a period of four years: (1)Power density spectra show strong red noise feature characterized by the steep power-law slopes of $\sim$ 2–3; (2) Structure functions suggest typical timescale of $\sim$ 0.5 days indicative of the duration of the successive flares; (3) Inter-band time lags differ from flare to flare and depend on photon energies. The soft lags may relate with the duration of the flares, in the sense that a flare with longer duration may show larger soft lag; (4) A trend that peak energies of synchrotron component increase with increasing fluxes is indicated; (5) Complexity of spectral evolution is detected with two flares track opposite directions in the soft and hard bands respectively, indicating changes of the sign of the time lags from the soft to hard energy band. The implications of our results are discussed in the context of synchrotron cooling model of relativistic electrons accelerated through internal shocks taking place in the jets of the source.

1. Introduction

It has been well established that blazars are extragalactic sources possessing relativistic jets aligned close to the line of sight. For high-energy (usually UV/soft X-rays) synchrotron peaked blazars (HBLs), X-rays provide an ideal radiative window for the study of the variations because (1) rapid variability indicates that the X-rays arise from the innermost region of the jets, and give direct clues on the central source; (2) synchrotron X-ray emission probes the electrons accelerated to the highest energies, which plausibly have the longest acceleration and shortest cooling times, and more complex variability patterns are expected in these sources. The detected TeV blazars so far are typical HBLs, including the three well-studied classical BL Lac objects, Mrk 421, Mrk 501, and PKS 2155–304. Because of their brightness, these sources have received particular attention as ideal targets for detailed temporal and spectral variability studies in the broadest spectral ranges. Extensive multiwavelength monitoring campaigns and intensive long looks with various satellites have been conducted to probe the dynamics and the structure of the jets. We present here the temporal and spectral characteristics of the X-ray emission of PKS 2155–304 from all the three long-looks with *Beppo*SAX during a period of four years. The journal of the observations is summarized in Table I.

2. Temporal Analysis

The light curves are shown in the left panel of Figure 1. It is clear that the source underwent pronounced brightness changes and showed significant variations with recurrent flares detected.

We first calculate the normalized power spectral density (NPSD) utilizing the standard discrete Fourier transform (e.g., Hayashida et al. 1998). Each light curve is rebinned over 5670 s and 256 s in order to obtain evenly sampled time series, from which the low- and high-frequency NPSD are estimated respectively (see Zhang et al. 2002 for details).

TABLE I
Observational Journal of PKS 2155–304 with *Beppo*SAX

Observing Time (UTC)	Duration (hour)	Net Exposure (ks) LECS	MECS
1996/11/20 00:15:58–1996/11/22 13:30:06	51.2	36.29	106.9
1997/11/22 16:03:00–1997/11/24 01:35:12	32.5	22.49	59.49
1999/11/04 04:27:27–1999/11/06 16:52:12	60.4	46.12	104.0

The combined NPSD in the 2–10 keV band of each light curve is shown in the rigth panel of Figure 1. It can been seen that each NPSD generally shows quick decrease of power with increasing frequency and can be fitted with a power-law model ($P(f) \propto f^{-\alpha}$). The behavior of strong *red noise* variability is indicated by the steep slopes ranging from $\sim$ 2 to 3.

We then calculate the first order normalized structure function (NSF; Simonetti, Cordes & Heeschen 1985)) in the 2–10 keV band of each light curve which is rebinned in 1000 s). The results are shown in the left panel of Figure 2. It can been seen that each NSF shows a characteristic timescale, τ_c, identified as the timescale where the first "turn-over" of the NSF occurs. In order to properly determine τ_c and the slope, we fit each SF with a broken power-law model (solid lines in the left panel of Figure 2). The results show that the power-law slopes of the SFs are $\sim$ 1–1.5, this corresponds to a NPSD power-law slope of $\sim$ 2–2.5, consistent with those from NPSD directly. Moreover, our results suggest τ_c being about half day characteristic of the duration of the flares.

Cross-correlation analysis using two techniques suited to unevenly sampled time series, the Discrete Correlation Function (DCF; Edelson & Krolik) and the Modified Mean Deviation (MMD; Hufnagel & Bregman 1992), are performed to evaluate the inter-band time lags of variations at different energies. The results focusing on the "single" flares show that the soft lag (lower energy photons lagging higher energy ones) of the source differs from flare to flare, ranging from a few hundred seconds to one hour or so. We further quantify the energy-dependence of the soft lags for the 1996 #2 and 1999 #1 and #2 flares which show obvious soft lags. The results are shown in the right panel of Figure 2.

3. Spectral Analysis

To reveal in detail the spectral evolution, we perform time-resolved spectral analysis with the continuously curved model (Fossati et al. 2000) to account for the X-ray spectral curvature in PKS 2155–304. The special features of the curved model are to find the energy at which the νF_ν spectrum peaks ($E_{\rm peak}$ of synchrotron component) and the local spectral index at desired energies. To do so, we divide each observation into sub-segments on the basis of single *Beppo*SAX orbit or a multiple of it to reach sufficient statistics for each segment.

The source revealed a large flux variability, a factor $\sim$ 10 in the 2–10 keV energy band, ranging from 15.1×10^{-11} (1997 maximum) to 1.8×10^{-11} (1999 minimum) erg cm^{-2} s^{-1}. Such flux changes were accompanied by changes of spectral curvature characterized by the shifts of the peak energy of synchrotron component as seen in the $\nu - \nu F_\nu$ diagram. Figure 3 shows the spectral energy distribution derived from the segment with the maximum flux of each observation, and the relation of $E_{\rm peak}$ versus the 2–10 keV flux. There is a suggestion that $E_{\rm peak}$ shifts to higher energy with increasing flux, but this trend is clearly dominated by the upper limits of $E_{\rm peak}$. This is because $E_{\rm peak}$ of PKS 2155–304 is very close to the lower energy limit of *Beppo*SAX.

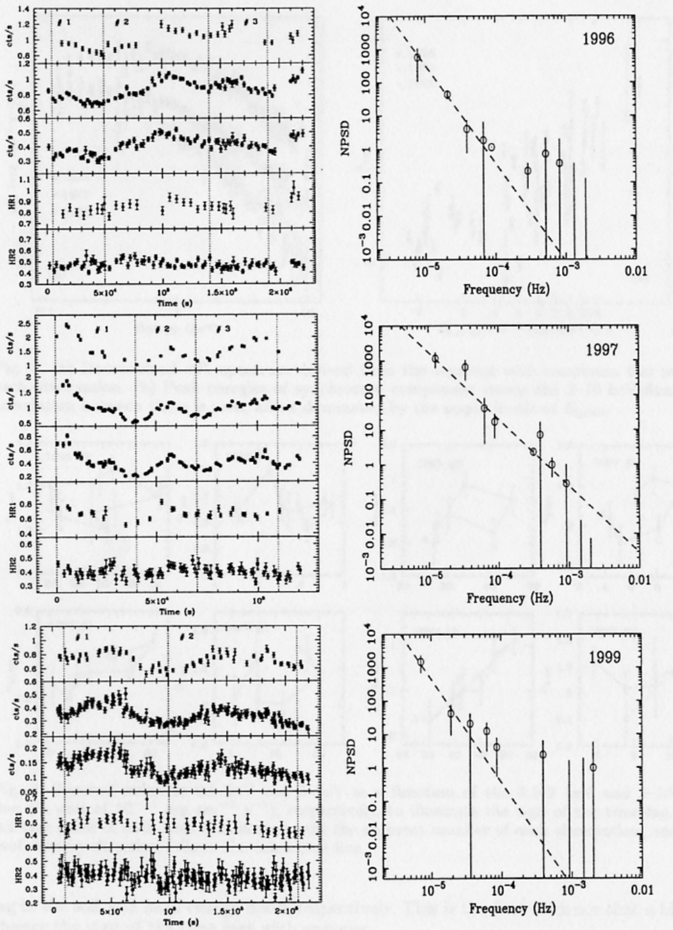

Fig. 1. Light curves (left) and the corresponding normalized power spectral density (NPSD) derived from the 2–10 keV band (right). From top to bottom is the 1996, 1997, and 1999 observation respectively. Each light curve (from top to bottom) shows the count rates in 0.1–1.5, 1.5–3.5 and 3.5–10 keV, and the hardness ratios of 1.5–3.5/0.1–1.5 (HR1) and 3.5–10/1.5–3.5 keV (HR2), respectively. "Single flares" are numbered. The dashed line of each NPSD corresponds to the best fit with a power-law model.

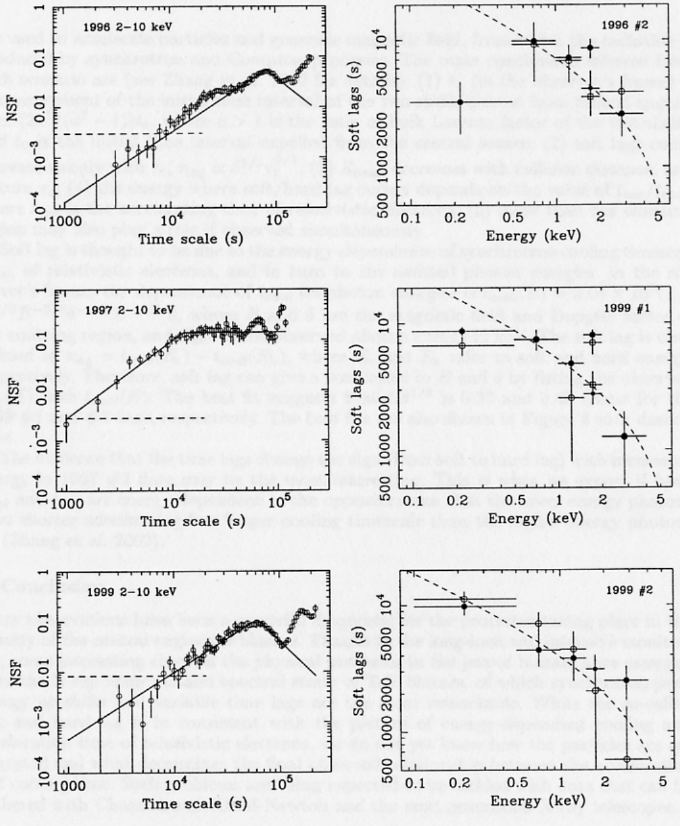

Fig. 2. (**Left**) Structure function of the 2–10 keV light curve. Solid lines are the best fit with a broken power law model, and the dashed line indicates the level of measurement noise. (**Right**) Soft lags as a function of photon energies for the 1996 #2, 1999 #1 and #2 flares as indicated in the light curves (Figure 1). The dashed line is the best fit with synchrotron cooling time which is energy-dependent.

We further probe spectral evolution on the plane of $\alpha - F$, and complex behaviors are found. Figure 4 plots the spectral index at 0.5 keV and 5 keV versus the 0.1–2 keV and the 2–10 keV absorption-corrected flux, respectively. Apart from the normal clockwise direction showing soft lag feature in both soft and hard energy band, the main flare of 1996 (#2) shows evidence of hard lag in the soft energy band and soft lag in the hard energy band. Moreover, 1997 #2 flare shows the opposite behavior, i.e., soft and hard

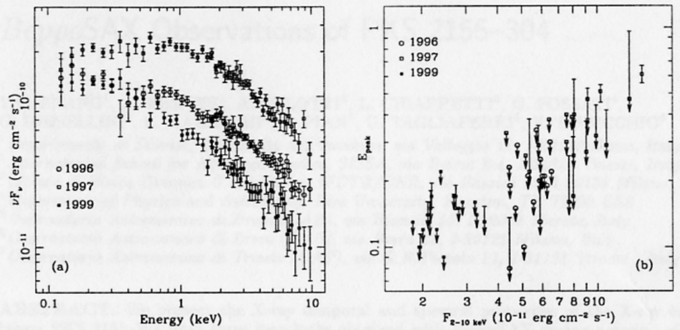

Fig. 3. (a) Deconvolved νF_ν spectrum derived from the segment with maximum flux among each observation. (b) Peak energies of synchrotron component versus the 2–10 keV fluxes. A correlation between them is seen, albeit dominated by the upper limits of $E_{\rm peak}$.

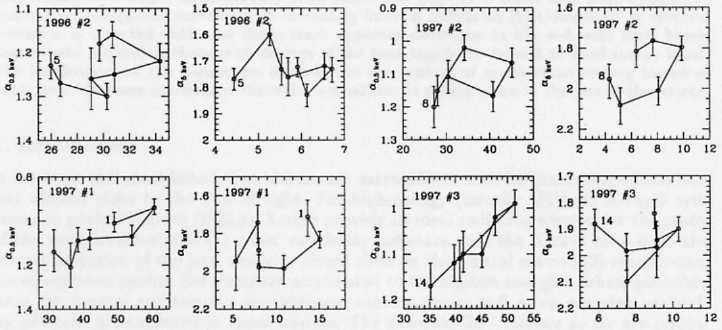

Fig. 4. Spectral index at 0.5 keV and 5 keV as a function of the 0.1–2 keV and 2–10 keV flux (in unit of 10^{-11} erg cm^{-2} s^{-1}), respectively, to illustrate the sign of the time lag. The starting point of each loop is indicated with the segment number of each observation, and the evolutionary direction follows the connected line.

lag in the soft and hard energy band, respectively. This is the first evidence that a blazar change the sign of the time lags with energies.

4. Discussion

We discuss our main findings, i.e., τ_c, soft lag and $E_{\rm peak}$, in line with the internal shock scenario in blazar jets (e.g., Spada et al. 2001). The key idea of this scenario is to assume that the central engine of a blazar is working in a intermittent rather than in a continuous way to expel discrete shells of plasma with slightly varying velocities. The shock will be formed due to collision when a later faster shell catches up a earlier slower one. The dissipation of bulk kinetic energy carried by the shells during shock period are used to accelerate particles and generate magnetic field, from which the radiation is produced by synchrotron and Compton processes. The main conclusions inferred from such scenario are (see Zhang et al. 2002 for details): (1) τ_c (in the observer's frame) is a measurement of the initial time interval of the two shells ejected from central engine, $\tau_c \simeq (2a^2/(a^2-1))t_0$, where $a > 1$ is the ratio of bulk Lorentz factor of the two shells, and t_0 is the initial time interval expelled from the central source; (2) soft lags could increase steeply with τ_c, $\tau_{\rm lag} \propto \delta^{5/2}\tau_c^{9/4}$; (3) $E_{\rm peak}$ decreases with collision distance, and in turn τ_c; (4) the energy where soft/hard lag occurs depends on the value of $t_{\rm acc}/t_{\rm cool}$, where $t_{\rm acc}$ is the accelerating time of relativistic electrons; (5) more than one emitting region may also play a role if observed simultaneously.

Soft lag is thought to be due to the energy-dependence of synchrotron cooling timescale, $t_{\rm cool}$, of relativistic electrons, and in turn to the emitted photon energies. In the observer's frame, the dependence of $t_{\rm cool}$ on photon energies is $t_{\rm cool}(E) = 3.04 \times 10^3 (1+z)^{3/2} B^{-3/2} \delta^{-1/2} E^{-1/2}$ s, where B and δ are the magnetic field and Doppler factor of the emitting region, and $E_{\rm keV}$ is the observed photon energy in keV. The soft lag is then defined as $\tau_{\rm lag} = t_{\rm cool}(E_{\rm s}) - t_{\rm cool}(E_{\rm h})$, where $E_{\rm s}$ and $E_{\rm h}$ refer to soft and hard energy, respectively. Therefore, soft lag can give a constraint to B and δ by fitting the observed $\tau_{\rm lag}(E)$ with $t_{\rm cool}(E)$. The best fit suggests that $B\delta^{1/3}$ is 0.37 and 0.40 Gauss for the 1999 #1 and #2 flare, respectively. The best fits are also shown in Figure 2 with dashed lines.

The evidence that the time lags change the sign (from soft to hard lag) with increasing energy in 1997 #2 flare may be the most interesting. This is what we expect if both $t_{\rm cool}$ and $t_{\rm acc}$ are energy-dependent in the *opposite* sense that the lower energy photons have shorter accelerating but longer cooling timescale than the higher energy photons do (Zhang et al. 2002).

5. Conclusion

X-ray observations have been a powerful diagnostic for the processes taking place in the vicinity of the central engines of blazars. Thanks to the long-look and intensive monitoring, some interesting clues on the physical processes in the jets of blazars have emerged from the X-ray temporal and spectral study of TeV blazars, of which synchrotron peak energy up-shifts and variable time lags are the most remarkable. While the so-called soft and hard lag is in consistent with the picture of energy-dependent cooling and acceleration time of relativistic electrons, we do not yet know how the particles are accelerated and what determines the final observed relationship between the acceleration and cooling time. Such problems are being expected to be tackled with data that can be gathered with Chandra and XMM-Newton and the next generation X-ray telescopes.

Acknowledgements

We greatly thank the *Beppo*SAX Science Data Center (SDC) for providing the standard event files archive. We acknowledge the Italian MUIR for financial support.

References

Edelson R.A., Krolik J.H.: 1988, *Astrophys. J.* **333**, 646.
Fossati G. et al.: 2000b, *Astrophys. J.* **541**, 166.
Hayashida K. et al.: 1998, *Astrophys. J.* **500**, 642.
Simonetti J.H., Cordes J.M., Heeschen D.S. 1985, *Astrophys. J.* **296**, 46.
Spada M. et al.: 2001, *Mon. Not. R. Astr. Soc.* **325**, 1559.
Zhang Y.H. et al: 2002, *Astrophys. J.* **572**, inpress (astro-ph/0202378).